Crack Mode in High Temperature Multiaxial Low Cycle Fatigue

M. SAKANE and M. OHNAMI
Department of Mechanical Engineering, Faculty of Science and Engineering, Ritsumeikan University, Kyoto, Japan

ABSTRACT

This paper describes the correlation of high temperature multiaxial low cycle fatigue life with different fracture mode. Crack opening displacement(COD) was analyzed by FEM for mode I, II and III cracks. The equivalent stress and strain based on the COD were developed and the applicability of these parameters was discussed.

KEYWORDS

Low cycle fatigue; Multiaxial stress; High Temperature; Fracture mechanics

INTRODUCTION

Studies of the biaxial/multiaxial fatigue are essential since most of structural components suffer more or less multiaxial fatigue damages. Recent studies(Hamada et al., 1985, Sakane et al., 1987) of high temperature multiaxial fatigue have cleared that the Mises' stress and strain, which have been most frequently used historically as a multiaxial fatigue failure parameter, are not necessarily appropriate for assessing the multiaxial low cycle fatigue life. These parameters in essential describe the strain energy accumulated in the specimen but the low cycle fatigue failure is determined by cracks. A more accurate multiaxial low cycle fatigue parameter is needed.

This paper challenges to clear what parameter is effective to correlate the multiaxial low cycle fatigue lives in mode I, II and III of a type 304 stainless steel at elevated temperatures. Fatigue failure lives are mostly spent in crack propagation life, so the parameters which correlate the crack propagation rate in multiaxial stress states are also described in the paper.

FAILURE ANALYSIS

The failure mode discussed in this paper is mode I, mode I with parallel stress to the crack, mode II and mode III. As is well known, mode I type failure occurs in the uniaxial push-pull test and the low cycle fatigue

data obtained in this test is considered as the basic data in design. To estimate the multiaxial low cycle fatigue life from the uniaxial fatigue data is necessary.

Parallel stress additionally applied to mode I crack significantly increases the crack propagation rate(Sakane et al., 1987, Hamada et al., 1987) When assessing the multiaxial fatigue life we could not ignore the contribution of the parallel stress. This type of failure occurs in the reversed torsion fatigue of the notched and precracked tubular specimens(Sakane et al., 1988). It is very interesting that for the precracked specimen the direction of the precrack has almost no effect on the post-crack direction. The macro crack always propagates in mode I regardless the precrack direction(Sakane et al., 1988). As the parallel stress increases the crack propagation rate and which results in the smaller fatigue life. So, analyzing the effect of parallel stress is important when discussing the biaxial fatigue life. Firstly this paper discusses the effect of the parallel stress on the crack behavior and failure life.

Figure 1(Sakane et al., 1987) shows the crack transition of the type 304 tubular smooth specimen at 923 K in the combined push-pull and reversed torsion test. The main crack direction changes from mode I to II as the principal strain ratio decreases, where the principal strain ratio is defined as $\varepsilon_3/\varepsilon_1$. For correlating the fatigue life between the push-pull and the reversed torsion tests, the failure parameter to connect both the failure modes is necessary. This paper secondly discusses the correlation of the reversed torsion fatigue life with the push-pull fatigue life considering the crack propagation behavior in two modes.

Smooth specimen	Δεeq (%)		
	1.5	1.0	0.7
Main crack	○	◑	◒
Sub crack(0l< l <10mm)	▽	▼	▽
Micro crack(l <0l mm)	△	▲	△

Notched specimen	Δε1 (%)		
	1.5	1.0	0.5
Main crack	□	◨	◪

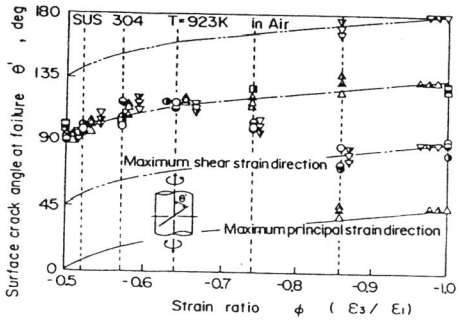

Fig.1 Crack direction of type 304 tubular smooth specimen in the combined push-pull and reversed torsion fatigue test at 823 K.

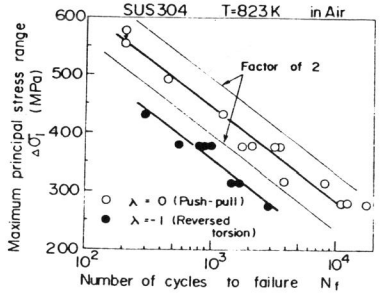

Fig.2 Correlation of the fatigue life between the push-pull and the reversed torsion using the maximum principal stress.

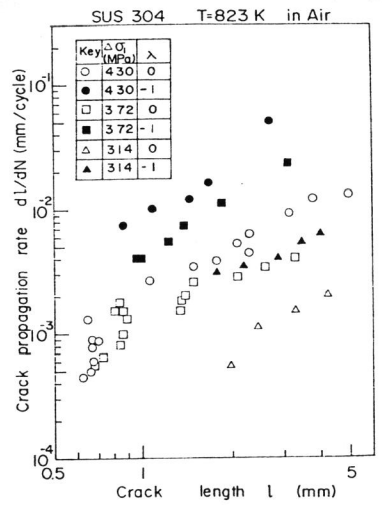

Fig.3 Comparison of the crack propagation rate between the push-pull and the reversed torsion tests.

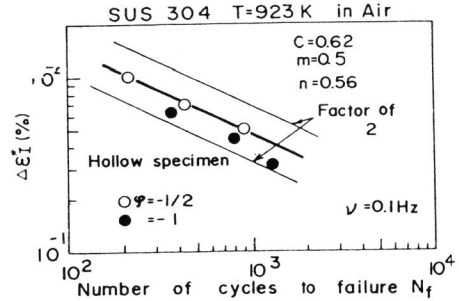

Fig.5 Correlation of the push-pull fatigue life with the reversed torsion fatigue life using the equivalent mode I COD strain.

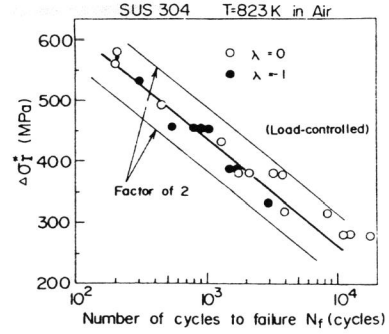

Fig.4 Correlation of the push-pull fatigue life with the reversed torsion fatigue life using the equivalent mode I COD stress.

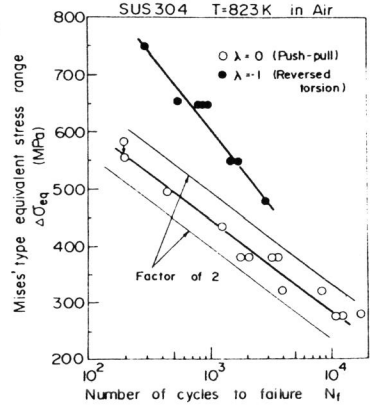

Fig.6 Correlation of the push-pull fatigue life with the reversed torsion fatigue life using the Mises' equivalent stress.

The last crack mode is mode III. To make an experiment to obtain the mode III fatigue failure life is very difficult so that only the mode III crack propagation life is discussed in the paper. The mode III crack propagation life was provided by conducting the reversed torsion fatigue using the circumferential notched solid specimen. The correlation of the crack propagation life between mode I and mode III is discussed.

EFFECT OF PARALLEL STRESS IN MODE I FATIGUE FAILURE LIFE

Figure 2(Hamada et al., 1985) shows the principal stress range-low cycle

fatigue life relation in the push-pull and reversed torsion test for a type 304 hollow cylindrical specimen with a 1-mm center notch hole at 823 K. The reversed torsion test exhibits the smaller fatigue life in comparison with the push-pull test. For both the tests, the specimen failures in mode I, so only the difference in the loading condition is the parallel stress to the crack in the reversed torsion test. Figure 3(Hamada et al., 1985) compares the crack propagation rate in the push-pull test with that in the reversed torsion test. The latter is larger than the former at the same principal stress, which shows that the parallel stress increases the crack propagation rate. The effect of the parallel stress should be properly taken account of for the biaxial low cycle fatigue life data correlation.

To take account of the parallel stress, the authors have proposed the crack opening displacement (COD) approach(Ohnami and Sakane, 1987). The COD approach is that the cracks exhibit the same propagation rate if they have the same COD amplitude. Conversely, if we can estimate the contribution of the parallel stress to the COD quantitatively, we can predict the crack propagation rate.

The authors have derived the equivalent stress which includes the contribution of the parallel stress to the COD(Hamada et al., 1985). The equivalent stress is expressed as

$$\Delta\sigma_1^* = \alpha\Delta\sigma_1(2-\lambda)^m \qquad \alpha = 1/\sqrt{2}, m=0.5 \qquad (1)$$

where σ_1 is the maximum principal stress, λ the principal stress ratio ($= \sigma_3/\sigma_1$) and α and m are the material constant. These material constants have the same value in the wide range of temperatures for the type 304 steel. Figure 4(Hamada et al., 1985) shows the correlation of the data shown in Fig.3 with the equivalent stress. The discrepancy of the data correlation between the push-pull and the reversed torsion tests is disappeared.

The COD strain, which also expresses the intensity of COD, can be also derived from the σ_1^* using continuum mechanics. The equation has the following form(Hamada et al., 1985).

$$\Delta\varepsilon_I^* = C\Delta\varepsilon_1(\varphi^2+\varphi+1)^{1/2}\left[(\varphi+2)\{3(\varphi^2+\varphi+1)\}^{-1/2}\left(\frac{3}{\varphi+2}\right)^m\right]^{1/n} \qquad (2)$$

where φ is the principal strain ratio and is expressed as $\varepsilon_3/\varepsilon_1$. The material constant m is the same value in Eq.(1), n is the cyclic strain hardening exponent of the material and C is 0.62. Figure 5(Hamada et al., 1985) correlates the strain controlled fatigue data with the equivalent COD strain. All the data locate inside a factor of two scatter band.

From the above discussion, the equivalent COD stress and strain which express the intensity of the crack opening displacement provides the satisfactory data correlation between the push-pull and the reversed torsion tests. So, we can conclude that these equivalent values are available to correlate the mode I type failure in biaxial stress condition. Besides the equivalent COD values, the data correlation using Mises' stress and strain was made. Only the correlation using the equivalent stress is shown in Fig.6(Hamada et al., 1985). The reversed torsion fatigue data locate far above the push-pull data so that the Mises' stress is not an appropriate parameter for the correlation. The Mises' strain gives almost satisfactory correlation but the reversed torsion fatigue data locate above the push-pull fatigue and they are just outside a factor of two scatter band(Sakane et al., 1987).

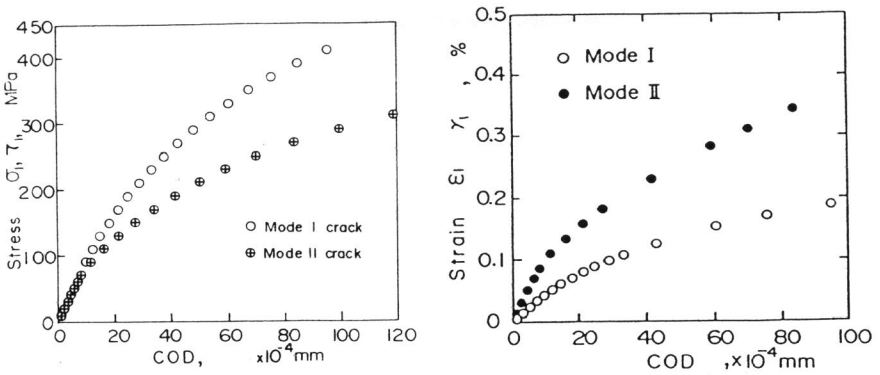

(a) Stress basis (b) Strain basis

Fig.7 Crack opening displacement for mode I and mode II cracks

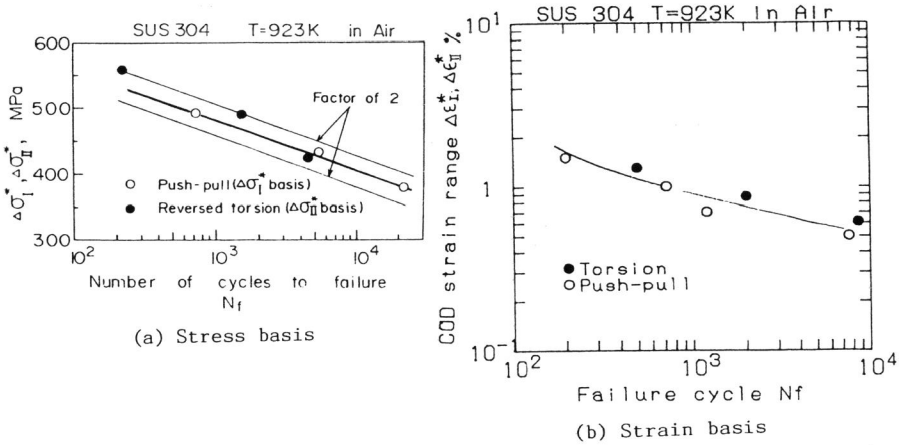

(a) Stress basis (b) Strain basis

Fig.8 Correlation of the fatigue life of the smooth specimen between the push-pull and the reversed torsion tests with the equivalent mode II COD parameters.

CORRELATION OF FATIGUE LIFE BETWEEN MODE I AND MODE II

The notched and precracked hollow cylindrical specimens fatigued in the reversed torsion fail by mode I crack but the smooth specimen in mode II(Sakane et al., 1988). In this case, the correlation of the fatigue failure data in mode I and mode II is necessary. Here, the authors also employ the COD approach. To calculate the COD amplitude, the FEM analysis was made for mode I and mode II cracks.

Figures 7 (a) and (b) show the results of the FEM analysis, where (a) is the stress basis while (b) the strain basis. As is well known, in the fully elastic range, the crack opening displacement in mode I agrees with that in mode II. In the analytical results in Fig.7, the CODs' in both the

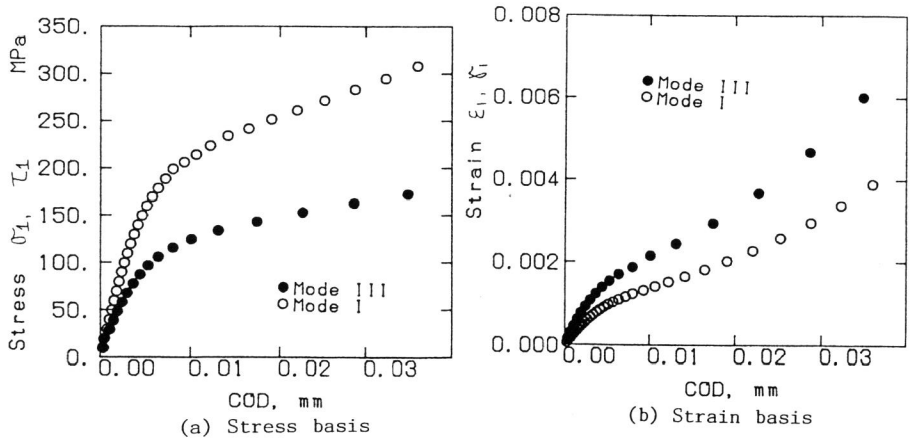

(a) Stress basis (b) Strain basis

Fig.9 Crack opening displacement in mode I and mode III cracks.

modes agree each other in the smaller stress range, but they begin to differ from each other as the applied stress increases. The COD in mode II is larger in comparison with mode I when the shear stress has the same stress amplitude as the normal stress. This means that, in the principal stress controlled test, the crack propagation rate in the reversed torsion becomes larger than that in the push-pull if the specimen fails by mode II crack in the reversed torsion test. The crack propagation rate of the smooth specimen in the push-pull and the reversed torsion tests is not available because of the difficulty of the experiment, so the fatigue failure lives in both the loading modes are compared with each other.

Before the comparison, we will derive the equivalent stress and strain in mode II which yield the same COD amplitude as mode I. From the ratios of σ_I/τ_I and ε_I/γ_I in the post yield condition, one can obtain the following relation.

$$\sigma_{II}^{*} = 1.4\,\tau_I \qquad \varepsilon_{II}^{*} = 0.5\,\gamma_I \tag{3}$$

Figures 8 (a)(Ohnami and Sakane, 1987) and (b) compare the push-pull low cycle fatigue data with the reversed torsion fatigue data. In the reversed torsion test, mode II failure occurred. The equivalent COD stress and strain quite well correlate the biaxial fatigue life so that we can conclude that the COD approach is available to the mode I and mode II data correlation.

CORRELATION OF FATIGUE LIFE BETWEEN MODE I AND III

Finally we will discuss the fatigue life correlation between mode I and mode III. Figures 9 (a) and (b) show the COD amplitudes against the normal and shear stress/strain in mode I and III. As well as the mode II, the same COD assumption for both the modes gives the following relation.

$$\sigma_{III}^{*} = 1.7\,\tau_I \qquad \varepsilon_{III}^{*} = 0.62\,\gamma_I \tag{4}$$

As the experiment to obtain the mode III low cycle fatigue failure data is difficult, the crack propagation life in mode III was compared with that in

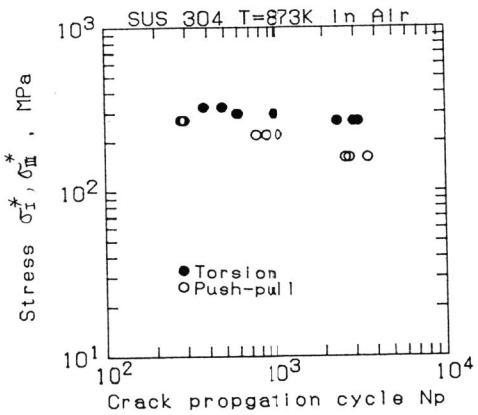

Fig.10 Correlation of the crack propagation life between mode I and mode III with the equivalent mode III COD stress.

mode I in this paper. The crack propagation life in mode III was generated by the reversed torsion fatigue for the circumferential notched solid specimen. Note that the low cycle fatigue failure life is significantly affected by the sharpness of the notch but the propagation life is not influenced by the sharpness of the notch(Sakane and Ohnami, 1986). So, the comparison of the crack propagation life made here is appropriate.

Figure 10 shows the correlation between the crack propagation lives in mode I and mode III. The specimen was type 304 stainless steel circumferential notched bar and the stress controlled fatigue test was carried out at 873 K. The notched specimen failured in mode I in the push-pull test but in mode III in the reversed torsion test. The correlation of the crack propagation life is good but the reversed torsion test exhibits the larger propagation life especially at the lower stress level, which may be attributed to the stress gradient in the reversed torsion test. The mode III strain controlled fatigue data was not available so the comparison using the strain parameter was not made here. The data correlation with the strain parameter is still an open question.

SUMMARY

The multiaxial low cycle fatigue parameters in mode I, II and III were derived from the FEM COD analysis and the correlation of the multiaxial fatigue data with these parameter was discussed. The summary of the effective parameter is listed in Table 1, where additionally the effective parameter, which is not discussed in this paper, is also added to the table.

Regarding the stress controlled fatigue, all the classical parameters such as Mises' equivalent stress, maximum principal stress, are not effective for the correlation of the multiaxial low cycle fatigue data. Only the equivalent stress based on the crack opening displacement is effective to the data correlation. As with the strain controlled fatigue, the COD strain is applicable to the correlation. The Mises' equivalent strain is

Table 1 Summary of the effective parameter to correlate the multiaxial fatigue life.

	Stress basis	Strain basis
Mode I	$\sigma_1=\sigma_{eq}=\sigma_I^*$	$\varepsilon_1=\varepsilon_{eq}=\varepsilon_I^*$
Mode I + Parallel stress	σ_I^*	ε_I^*, ε_{eq}
Mode II	σ_{II}^*	ε_{II}^*, ε_{eq}
Mode III	σ_{III}^*	(ε_{III}^*, ε_{eq})

( ):Not confirmed with experimental data.

also applicable if we permit a slightly larger scatter of the data. Only for the mode III strain controlled fatigue, the confirmation to the experimental results was not made because of the unavailability of the experimental data.

REFERENCES

Hamada, N., Sakane, M., and Ohnami, M.(1985). A Study of High Temperature Low Cycle Fatigue Criterion in Biaxial Stress State. Bull. Japan Soc. Mech. Eng., 28, 1341-1347.

Hamada, N., Sakane, M., and Ohnami, M.(1987). Effect of Temperature on Biaxial Low Cycle Fatigue Crack Propagation and Failure Life of an Austenitic Stainless Steel. Proc. 30th Japan Congr. Mater. Res., 69-75.

Ohnami, M., and Sakane, M.(1987). Crack Propagation Rate and Failure Life in Biaxial Low Cycle Fatigue at Elevated Temperatures. Eng. Fract. Mech., 28, 699-709.

Sakane, M., Ohnami, M.(1986). Notch Effect in Low-Cycle Fatigue at Elevated Temperatures-Life Prediction From Crack Initiation and Propagation Considerations. J. Eng. Mater. Tech., 108, 48-54.

Sakane, M., Ohnami, M. and Sawada, M.(1987). Fracture Modes and Low Cycle Biaxial Fatigue Life at Elevated Temperature. J. Eng. Mater. Tech., 109, 236-243.

Sakane, M., Ohnami, M., and Hamada, N.(1988). Biaxial Low Cycle Fatigue for Notched, Cracked and Smooth Specimens at High Temperatures. J. Eng. Mater. Tech., 110, 48-54.